Original Research

Construction of an Immunity and Ferroptosis-Related Risk Score Model to Predict Ovarian Cancer Clinical Outcomes and Immune Microenvironment

Chunyan Wei[1,*], Gang Zhao[1], Mei Gao[1], Yunting Liu[2], Pan Lei[1], Ting Cao[1]

[1]Department of Gynaecology and Obstetrics, The Second Affiliated Hospital of Xi'an Jiaotong University, 710004 Xi'an, Shaanxi, China
[2]Department of Gynaecology and Obstetrics, Shangluo Central Hospital, 726000 Shangluo, Shaanxi, China
*Correspondence: chunyan_weisx@163.com (Chunyan Wei)
Academic Editor: Gea Oliveri Conti

Abstract

Background: Ovarian cancer (OV) is a severe and common gynecological disease. Ferroptosis can regulate the progression and invasion of tumors. The immune system is a decisive factor in cancer. The present study aimed to use gene expression data to establish an immunity and ferroptosis-related risk score model as a prognostic biomarker to predict clinical outcomes and the immune microenvironment of OV. **Methods**: Common gene expression data were searched from the Gene Expression Omnibus and The Cancer Genome Atlas databases. Immunity-related genes and ferroptosis-related genes were searched and downloaded from the ImmPort and FerrDb databases, followed by the analysis of the overall survival of patients with OV and the identification of genes. Subsequently, the status of the infiltration of immune cells and the association between immune checkpoints and risk score were assessed. **Results**: A total of 10 prognostic genes (*C5AR1*, *GZMB*, *IGF2R*, *ISG20*, *PPP3CA*, *STAT1*, *TRIM27*, *TSHR*, *RB1*, and *EGFR*) were included in the immunity and ferroptosis-related risk score model. The high-risk group had a higher infiltration of immune cells. The risk score, an independent prognostic feature of OV was negatively associated with each immune checkpoint. The risk score may thus help to predict the response to immunotherapy. **Conclusions**: The immunity and ferroptosis-related risk score model is an independent prognostic factor for OV. The established risk score may help to predict the response of patients to immunotherapy.

Keywords: immunity; ferroptosis; ovarian cancer; signature genes; prognosis; tumor immune microenvironment; immune checkpoint; immunotherapy

1. Introduction

Ovarian cancer (OV) is a severe and common gynecological disease, which often leads to mortality. It causes ~150,000 deaths each year, severely endangering women's health and safety [1,2]. OV-associated mortality ranks first in mortality from gynecological tumors [3]. Moreover, due to the early non-specific symptoms, 75% of women with OV are diagnosed at an advanced stage, and the majority of patients relapse following treatment [4]; in addition, the survival rates are not satisfactory [5]. Hence, it is necessary to identify reliable prognostic models for patients with OV [6–8]. However, the single-gene/factor prediction model is often less accurate. In comparison, the polygenic model generally yields better results in tumor prediction [9]. Thus, the subset of patients with a poor survival can be more accurately identified for more rigorous follow-up and post-treatment adjuvant therapy, which may aid in decision-making and individualized treatments.

Iron is a trace element required by the human body; thus, a lack or excess in iron can have multiple effects on biological processes [10]. Iron deficiency affects cancer cell proliferation [11]. However, it is worth noting that high iron concentrations cause cell death through membrane lipid peroxidation, which is known as ferroptosis [12]. Basuli *et al*. [13] reported that abnormal iron accumulation in high-grade serous OV tissue was significantly higher than that in normal OV tissue. In addition, iron transport-related genes have also been shown to be dysregulated in a genetic model of OV primary cells. The activation of ferroptosis is associated with progressive disease, and ferroptosis regulates the occurrence, progression and invasion of OV [14]. Ferroptosis may influence the progression of OV by mediating tumor metastasis and the immune landscape.

The immune system, a critical system in the human body, is a decisive factor in the occurrence and progression of cancer [15,16]. There is evidence to indicate that OV is an immunogenic tumor [17–19]. Immunotherapy is effective in treating human malignancy [20]. It has been reported that the phenotypes and functions of immune cell subsets in the OV microenvironment are altered by immunotherapy [21].

There are complex mechanisms of action between immunity and ferroptosis. For example, T-cells induce ferroptosis in ovarian tumor-bearing mice [22]. Based on the association between immunity, ferroptosis and OV, in the present study, mRNA analysis data were used to establish an immunity and ferroptosis risk score model to predict the

immune microenvironment of OV. In the future, this approach may aid clinicians in making important treatment-related decisions.

2. Materials and Methods

2.1 Data Set Sources and Preprocessing

Common gene expression data were obtained from the Gene Expression Omnibus (GEO) and The Cancer Genome Atlas (TCGA) databases. In TCGA dataset, RNA sequencing data for gene expression were downloaded from UCSC Xena. For the three datasets of GSE26712, GSE32062 and GSE18521, RNA sequencing data were downloaded from the easyGEO dataset. Among these, TCGA dataset was used as the training set, and the GEO dataset was used as the validation set. The details of the datasets are presented in Table 1, including number of patients, overall survival (OS), tumor stage, and tumor grade.

2.2 Identification of Immunity and Ferroptosis-Related Genes

Immunity-related genes (IRGs) were obtained from the immunology and ImmPort databases. A comprehensive gene list (involving 1793 IRGs) was downloaded. Ferroptosis-related genes (FRGs) were obtained from the FerrDb database and the related literature [23]. The FerrDb database is the first database that provides updated data of regulators and markers connected with ferroptosis and disease. Finally, 267 FRGs were obtained, including 259 FRGs from the FerrDb database, and 8 genes from the literature [23] as a complement.

2.3 Construction of an Immunity and Ferroptosis-Related Risk Score Model

According to the data of the TCGA training set and the GSE26712 validation set, the IRGs and FRGs were screened using univariate Cox analysis. The intersection of the genes in the two datasets was considered as the prognosis-related genes ($p \leq 0.05$). The least absolute shrinkage and selection operator (Lasso) method was applied to calculate the coefficient (β) to screen prognostic genes in TCGA dataset for reducing the number of genes in the risk score model. Eventually, the multivariate Cox regression analysis was applied to construct the risk score model. The calculation formula was as follows: Risk score = (βA × gene A expression) + (βB × gene B expression) + ⋯ + (βN × gene N expression).

In this formula, βA, βB...βN represent the coefficients of genes. Genes from which the risk score was constructed were defined as signature genes. The patients were then divided into high- and low-risk groups using the median risk score as the cut-off point. Survival curves were then plotted using Kaplan-Meier from R package (version 3.5.3). Accuracy was verified by time-dependent receiver operating characteristic (ROC) curves.

2.4 Molecular Characterization of Signature Genes

The signature genes in each sample were divided into the high- and low-expression groups according to the median expression in TCGA dataset. Kaplan-Meier analysis was applied to analyze the influence of signature genes on survival. The expression of signature genes in cancer and paracancerous tissues was searched from the Gene Expression Profiling Interactive Analysis (GEPIA) database and verified in the GSE26712 and GSE18521 datasets. At the same time, the Human Protein Atlas database was applied to detect the protein expression of signature genes in cancer tissues.

2.5 In Vitro Expression Analysis of Signature Genes Using Real Time Polymerase Chain Reaction (RT-PCR)

To further validate the expression of signature genes at the mRNA level, RT-PCR assays were performed using the tissue samples. Tumor tissues and paracancerous tissues were collected from 8 patients with OV. The clinical data of the patients are provided in detail in Table 2, mainly including age, tumor size, stage, grade, tumor metastasis, alcohol, smoking and family history. In addition, the increase of CA125, HE4 and CA199 suggests the possibility of malignancy.

The inclusion criteria for the patients with OV were as follows: (1) Patients were diagnosed with OV for the first time; (2) patients had not undergone other treatments prior to diagnosis; (3) patients had no other malignancy; (4) patients had no other autoimmune disease; (5) the age of the patients was 18 to 70 years. The exclusion criteria were as follows: (1) Patients had other malignancies; (2) patients received other treatments prior to surgery; (3) patients had incomplete clinical data; (4) patients had a history of cancer. The Ethics Committee of The Second Affiliated Hospital of Xi'an Jiaotong University approved this study (2021241). Patient informed consent was obtained.

RNA was extracted from the tissue samples. The SYBR-GreenIReal Time PCR method was used to detect the changes in gene expression. Relative gene expression values were determined using the $2^{-\Delta\Delta ct}$ method (compared to healthy controls). $2^{-\Delta\Delta ct} > 1$ and $2^{-\Delta\Delta ct} < 1$ represent up- and downregulation, respectively. *ACTB* was used as an internal reference gene.

2.6 Drug Predictions of Signature Genes

Based on the DGIdb database (https://dgidb.org/), those drugs related to signature gene were screened out, which may provide new perspectives for OV diagnosis, treatment and research.

2.7 Association of Risk Score with Clinical Feature

For the purpose of further investigating the association between clinical features of OV and risk score, univariate and multivariate Cox analysis were first applied to determine the independent prognostic factors of the risk score

<div align="center">**Table 1. Basic information of datasets.**</div>

Accession number	Platform	Number of normal controls	Number of patients	OS (years)			Tumor stage					Tumor grade				
				1/4 quartile	Median	3/4 quartile	I	II	III	IV	Other	1	2	3	4	Other
GSE26712	GPL96	10	185	1.81	3.19	5.15	0	0	144	41	0	0	0	40	144	1
GSE32062	GPL6480	0	260	2.22	3.41	4.68	0	0	204	56	0	0	0	131	129	0
GSE18521	GPL570	10	53	N/A	N/A	N/A		late					high			
TCGA	Illumina RNAseq	0	378	1.44	2.81	4.55	1	23	294	57	3	1	45	321	1	10

OS, overall survival.

<div align="center">**Table 2. Clinical Information Registry.**</div>

Number	Age (years)	Tumor size (cm)	CA125 (U/mL)	HE4 (pmol/L)	CA199 (U/mL)	Roma index (%)	Tumor stage	Tumor grade	Tumor metastasis	Alcohol history	Smoking history	Family history of OV
1	58	1	811.6	96.10	7.94	82.66	IIIB	G3	Yes	No	No	No
2	62	10	305	58.86	19.18	58.31	IA	G1	No	No	No	No
3	70	8	631.3	736.7	7.94	97.06	IIIC	G3	Yes	No	No	No
4	73	20	982.6	>1500	5.18	98.96	IIIC	G3	Yes	No	No	No
5	56	10	148	51.65	10.8	15.29	IA	G1	No	No	No	No
6	47	12	437.9	219.9	4.65	77.14	IIIC	G2-G3	Yes	No	No	No
7	61	15	766.2	184.9	<0.6	60.63	IIIB	G1	Yes	No	No	No
8	52	15	60.34	128.1	24.61	48.95	IIIA	G2-G3	Yes	No	No	No

CA125, carbohydrate antigen 125; HE4, human epididymis protein 4; CA199, Carbohydrate antigen199; Roma index, Risk of Ovarian Malignancy Algorithm index; OV, ovarian cancer.

different from other clinical factors. After testing for collinearity, the independence of risk was also verified. All independent prognostic parameters and associated clinical parameters were applied to construct prognostic nomograms through stepwise Cox regression models to predict the overall survival (OS) of patients with OV. A nomogram was used to forecast the OS. In addition, differences in risk score in the various clinical subgroups were compared.

2.8 Analysis of Tumor Immune Microenvironment (TIME) Cell Infiltration

The relative abundance of each cell infiltration in the TIME of OV was quantified using single-sample Gene Set Enrichment Analysis (ssGSEA). In the study by Charoentong, gene sets that marked each immune cell type infiltrating the TIME, which is enriched in multiple human immune cell subtypes, were obtained [24,25]. The stromal score, tumor purity and ESTIMATE score of each patient with OV were calculated using ESTIMATE from R package (version 3.5.3). The Wilcoxon test was applied to compare the differences in immune cell infiltration, stromal score, tumor purity and the ESTIMATE score.

2.9 Gene Set Variation Analysis (GSVA)

Differences in biological processes were investigated using GSVA between the high- and low-risk groups. "C2.cp.kegg.v7.2.Symbols" was downloaded from the Molecular Signature Database. The R package "limma" was applied to calculate significantly enriched pathways. A false discovery rate (FDR) <0.05 was considered as statistically significant.

2.10 Gene Ontology (GO) Analysis

The R package "limma" was applied to identify differentially expressed genes (DEGs) between the high- and low-risk groups under the screening thresholds of FDR <0.05 and $|\log_2(FC)|$ >0.5. The Database for Annotation, Visualization and Integrated Discovery (DAVID) was applied to perform enrichment analysis, and the screening threshold was FDR <0.05.

2.11 Tumor Mutation Burden (TMB) Analysis

First, the "maftools" package in R was utilized to calculate the TMB score. Tumor samples were divided into the high- and low-TMB groups based on the median of TMB. The survival curve between risk and TMB was analyzed using the Kaplan-Meier method. In addition, a correlation analysis between the risk score and TMB was performed.

2.12 Immune Checkpoints and Immunotherapy

For the purpose of exploring the predictive power of tumor risk score in patients treated with immunotherapy, the expression of multiple immune checkpoints was assessed in the high- and low-risk groups and their correlation with the risk score was determined. Based on immunotherapy

cohorts, the responses of patients were analyzed in the high- and low-risk groups. The difference in the risk score in the response and non-response groups was analyzed.

2.13 Statistical Analysis

Based on the clinical data of OV cases in TCGA and the GEO datasets, univariate Cox proportional hazards regression analysis was used to screen genes associated with immunity and ferroptosis for survival ($p < 0.05$). The Lasso method was used to screen variables to prevent over-fitting and build a prognostic model. Survival curves for risk score were analyzed using Kaplan-Meier analysis, and the 1-, 3-, and 5-year time ROC curves of the model were plotted using the R package "timeROC". Univariate and multivariate Cox analyses were used to determine whether risk was an independent prognostic factor distinct from other clinical factors. Statistically significant differences were assessed using the two-tailed t-test in the RT-PCR experiments. The ssGSEA algorithm was used to quantify the relative abundance of each cell infiltration in the OV TIME, and the stromal score, tumor purity and the ESTIMATE score were calculated for each patient with OV using the ESTIMATE algorithm through the R package "ESTIMATE". In addition, based on the Wilcoxon test, the differences in various immune cells, stromal scores, tumor purity and the ESTIMATE score between the high- and low-risk groups were compared. In addition, the correlation between key genes and immune cells was explored based on Pearson's correlation analysis. GSVA enrichment analysis was performed using the R package "GSVA" and based on the R package "limma" was used to calculate differentially expressed pathways (FDR <0.05). DEG analysis was performed using the R package "limma" between the high- and low-risk groups (FDR <0.05 and $|\log_2(FC)|$ >0.5). Multiple testing correction was performed in the GSVA and GO enrichment analysis in the high- and low-risk groups. An FDR <0.05 was considered statistically significant. DAVID was used for the enrichment analysis of DEGs between the high- and low-risk groups (FDR <0.05). TMB was calculated using the "maftools" package in R.

3. Results

3.1 Construction of an Immunity and Ferroptosis-Related Risk Score Model

To investigate the impact of immunity and ferroptosis genes on the prognosis of patients with OV, univariate Cox regression analysis was applied in TCGA and the GSE26712 datasets with a screening criterion of $p \leq 0.05$; a total of 220 and 118 genes were identified. After taking the intersection of the genes in the two datasets, 12 prognostic genes were finally identified (Fig. 1), including *C5AR1*, *COLEC12*, *EGFR*, *GZMB*, *IGF2R*, *ISG20*, *PPP3CA*, *RB1*, *STAT1*, *TAP1*, *TRIM27* and *TSHR*.

Given the possible interaction between immunity and ferroptosis, 12 prognostic genes were used for the construc-
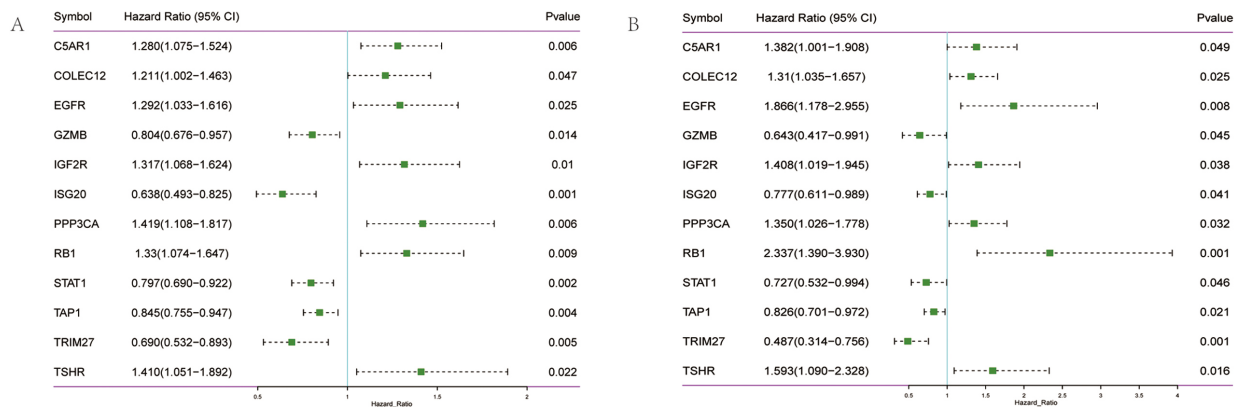
Fig. 1. Screening of prognostic genes in OV. (A) Forest diagram of 12 prognosis-related genes in TCGA training set. (B) Forest diagram of 12 prognosis-related genes in the GEO validation set.

tion of the prediction model of OV. The optimal λ (lambda) was obtained by the minimum partial likelihood deviation. Finally, 10 signature genes were obtained, including 8 immunity-related genes (*C5AR1*, *GZMB*, *IGF2R*, *ISG20*, *PPP3CA*, *STAT1*, *TRIM27* and *TSHR*), 1 ferroptosis-related gene (*RB1*) and 1 immunity and ferroptosis-related gene (*EGFR*). The immunity and ferroptosis-related risk score model was constructed, as shown in Fig. 2A,B. The formula is as following:

Risk score = (C5AR1 $\times$ 0.167018542) + (EGFR $\times$ 0.024944649) + (GZMB $\times$ –0.114825674) + (IGF2R $\times$ 0.223153693) + (ISG20 $\times$ –0.145695011) + (PPP3CA $\times$ 0.137679588) + (RB1 $\times$ 0.176152429) + (STAT1 $\times$ –0.157629949) + (TRIM27 $\times$ –0.446534567) + (TSHR $\times$ 0.14287582)

The influence of the risk score obtained from the construction of 10 immunity and ferroptosis-related genes on OS was further investigated. The risk score was calculated using a formula (detailed results are presented in **Supplementary Table 1**), the samples were divided into the high- and low-risk groups based on the median risk score. The low-risk group had a higher survival proportion, as shown in Fig. 2C. The OS was significantly lower in patients in the high-risk group (Fig. 2D). The AUC values at 1, 3 and 5 years were 0.639, 0.645 and 0.716, respectively (Fig. 2E). In TCGA training set, the risk score had good predictive power for the OS of patients.

To further evaluate the robustness of the risk score in predicting the OS of patients with OV, two datasets (GSE26712 and GSE32062) were applied to test the prediction capacity of the risk score for OS. First, the risk scores of the tumor samples in the two datasets were calculated separately using the same formula. The samples were divided into the high and low-risk group based on the median risk score (**Supplementary Fig. 1A,D**). The low-risk group had a higher OS rate. The OS of the patients in the high-risk group was significantly lower (**Supplementary Fig. 1B,E**). In the GSE26712 dataset, the AUC values were 0.713, 0.73 and 0.731 at 1, 3 and 5 years, respectively (**Supplementary**

Fig. 1C). In the GSE32062 dataset, the AUC values were 0.643, 0.620 and 0.629 at 1, 3 and 5 years, respectively (**Supplementary Fig. 1F**). In the validation set, it was further demonstrated that the risk score model had a better predictive ability for patients with OV.

3.2 Influence of Signature Genes on OS

The results of survival analysis with the risk score revealed that the OS of the high-risk group was significantly lower than that of the low-risk group. Based on the expression values of signature genes in each sample of the TCGA training set, the samples were divided into the high- and low-expression groups according to the median expression. The influence of signature genes on survival was analyzed using the Kaplan-Meier method. The *C5AR1*, *EGFR*, *RB1* and *TSHR* genes had no significant effect on survival ($p > 0.05$), while patients with a high expression of *GZMB*, *ISG20*, *STAT1* and *TRIM27* had a longer OS. In addition, patients with a low expression of *IGF2R* and *PPP3CA* had a longer OS (**Supplementary Fig. 2**).

Since there were no data available for the control group in TCGA dataset, the expression of signature genes in cancer and paracancerous tissues was searched from the Gene Expression Profiling Interactive Analysis (GEPIA) database. *STAT1* and *GZMB* were highly expressed in patients with OV, while *EGFR* was expressed at low levels in patients with OV. No significant differences were found for the remaining genes examined (Fig. 3). Subsequently, the expression of 10 signature genes was verified in the GSE26712 and GSE18521 datasets. *GZMB*, *ISG20* and *TSHR* were significantly upregulated in patients with OV, while *EGFR*, *PPP3CA* and *RB1* in GSE26712 were significantly downregulated in patients with OV. In the GSE18521 dataset, *C5AR1* was significantly expressed at low levels in patients with OV, while *GZMB*, *ISG20*, *STAT1*, and *TSHR* were significantly highly expressed in patients with OV (**Supplementary Fig. 3**). Of note, *GZMB* was significantly highly expressed in patients with OV in all data analyzed.

Fig. 2. Construction of risk model in TCGA training set. (A) Change trajectory of each independent variable. The horizontal axis and vertical axis represents the log value of the independent variable lambda and the coefficient of the independent variable, respectively. (B) LASSO Cox regression with 10-time cross-validation for optimal parameter (λ) selection, in which the vertical dashed lines showed minimum λ value and $1 \times$ standard error λ value, respectively. (C) Risk score distribution map, the dotted line indicates the optimal cut-off value of the risk score. All OV patients are divided into high and low risk groups. In survival status, the blue dots represent the surviving OV patients and the red dots represent death, and the corresponding risk gene cluster expression profiles were visualized as a heatmap. (D) Survival Curve, blue represents low risk score, red represents high risk score. (E) The yellow, blue and red lines represent 1, 3 and 5 years of the ROC curve, respectively.

At the same time, the Human Protein Atlas database was applied to analyze the protein expression levels of STAT1, GZMB and EGFR (**Supplementary Fig. 4A**). Based on the analysis using the UALCAN database, no significant expression difference was observed for STAT1; however, EGFR and PPP3CA proteins were expressed at low levels in patients with OV (**Supplementary Fig. 4B–D**).

In addition, RT-PCR detection indicated that *GZMB*, *STAT1* and *ISG20* were markedly upregulated in patients with OV (**Supplementary Fig. 4E**). The OS analysis with individual signature genes revealed that a high expression of the *GZMB*, *STAT1*, *ISG20* and *TRIM27* genes, and a low expression of the *IGF2R* and *PPP3CA* genes corresponded to a longer OS rate. However, the analysis of signature genes in cancer and paracancerous tissues revealed that the
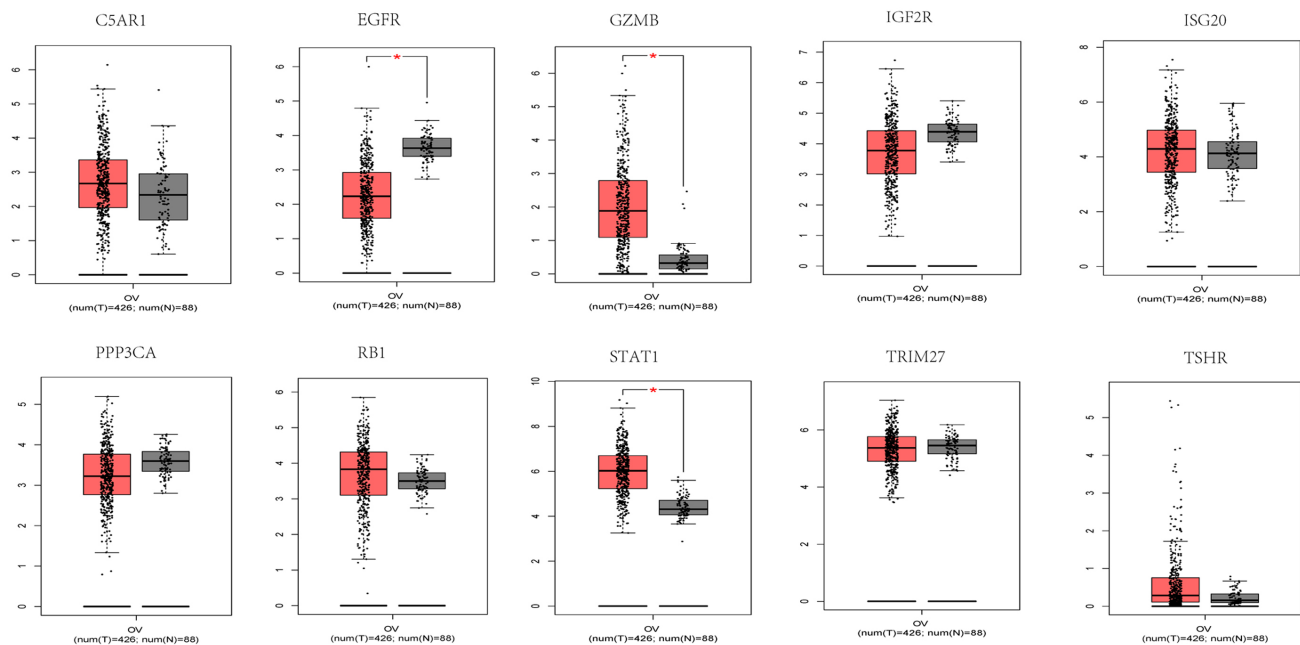
Fig. 3. Signature genes expression of *C5AR1*, *GZMB*, *IGF2R*, *ISG20*, *PPP3CA*, *STAT1*, *TRIM27*, *TSHR*, *RB1*, and *EGFR* in the GEPIA database. Red and gray represent the patients with tumor group and normal control group (T: tumor; N: normal control), respectively. $^*p < 0.05$.

GZMB, *STAT1* and *ISG20* genes still had higher expression levels, and that the *EGFR* and *PPP3CA* genes had lower expression levels in cancer tissues.

3.3 Drugs Predictions of Signature Genes

Based on the DGIdb database, drugs related to anti-tumor and immunotherapy for 10 signature genes were screened out (**Supplementary Fig. 5**), including 32 drugs and 4 genes (*EGFR*, *PPP3CA*, *RB1* and *STAT1*). Among these, cisplatin is widely used in the treatment of various solid tumors [26]. Sunitinib is a novel, multi-targeted oral treatment for cancer. Etoposide, docetaxel and decitabine are cell cycle-specific antitumor agents. Topotecan is indicated for metastatic advanced OV that has failed chemotherapy. Paclitaxel, vorinostat and other drugs are associated with OV treatment [27,28].

3.4 Independent Prognosis for OV

Univariate and multivariate Cox analyses determined the association of the risk score with clinical signatures. Age and risk could be used as independent prognosis factors (Fig. 4A). The independence of risk was verified in the validation set (Fig. 4B). A nomogram was constructed to predict OS probabilities by combining risk and age with significance for independent prognostic indicators in a multivariate Cox analysis (Fig. 4C,D). Each factor was allocated proportionally to its risk contribution to survival. The calibration curve indicated that the combined model (nomogram) revealed a high accuracy in OS at 1 year. In addition, differences in risk scores across clinical subgroups were compared. The risk scores significantly differed by age, status and stage (Fig. 4E).

3.5 Association of Risk Score with Immune Cell Infiltration

The infiltration status of 23 immune cells in TCGA dataset was evaluated using ssGSEA. The majority of the immune cells in the high-risk group had more infiltration (Fig. 5A). However, there was no corresponding survival advantage for patients in the high-risk group, and the OS of patients in the high-risk group was significantly lower (Fig. 2D). Epithelial-mesenchymal transition (EMT) 1, EMT2 and EMT3 was significantly higher in the high-risk group subtypes (Fig. 5B). Moreover, the ESTIMATE score, stromal score and tumor purity for each patient with OV was calculated using ESTIMATE. The ESTIMATE score and stromal score were significantly higher in the high-risk group, although tumor purity was low (Fig. 5C–E).

Furthermore, the ferroptosis status was also predicted based on suppressor genes (SOFs) and activators (DOFs) of ferroptosis in the literature [29]. Among the 16 repressors of ferroptosis, *CD44* and *HMOX1* were significantly highly expressed in the high-risk group, while *HELLS*, *HSF1*, *HSPA5*, *NQO1*, *OTUB1* and *SLC7A11* were significantly expressed at low levels. In the 22 ferroptosis activators, *ANO6*, *EGFR* and *ZEB1* were significantly highly expressed in the high-risk group, and *CHAC1*, *ELAVL1*, *PEBP1* and *SAT1* was significantly expressed at low levels. Taken together, the findings indicated that ferroptosis may be more pronounced in the high-risk group
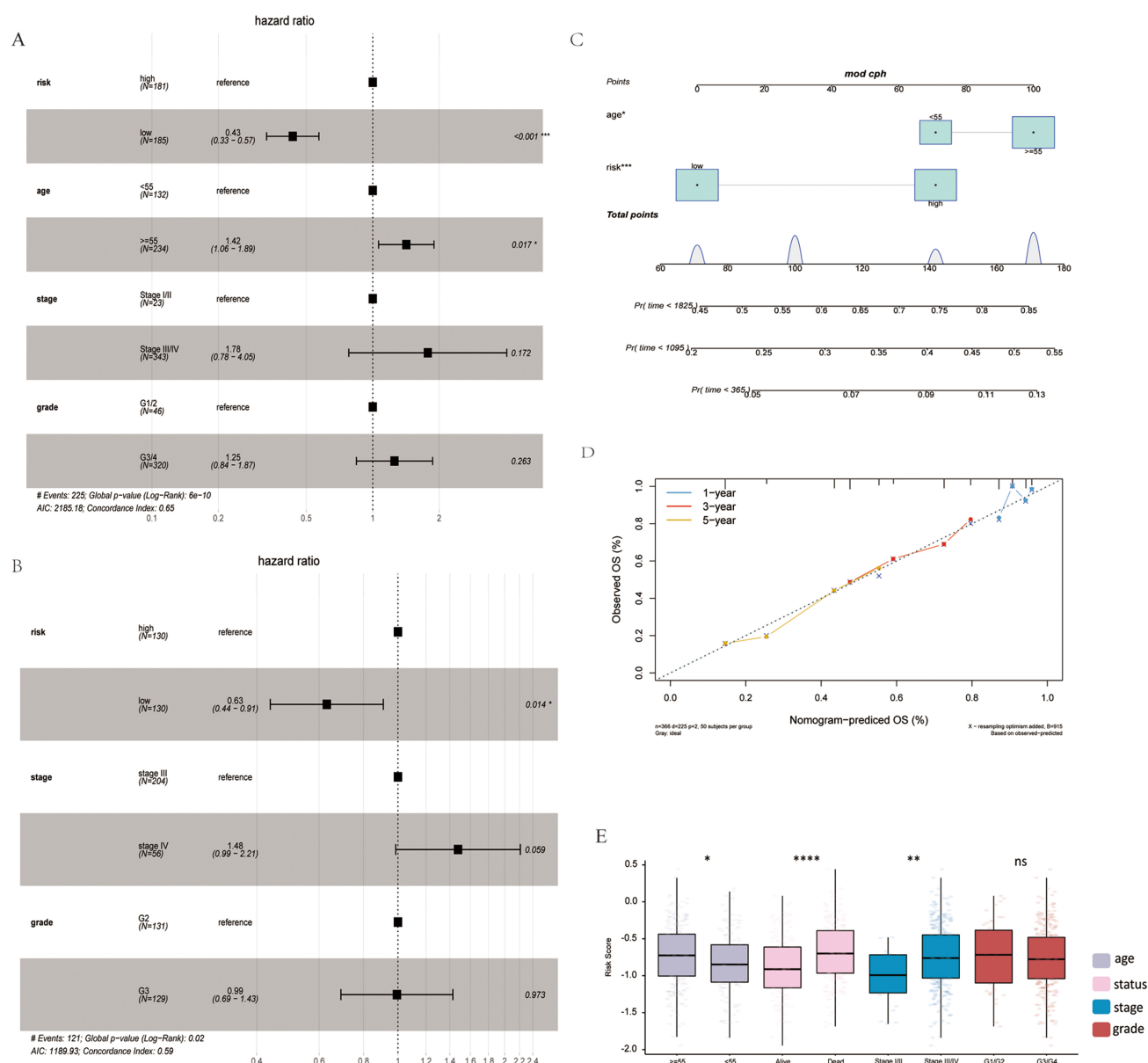
Fig. 4. Association of risk score with clinical features. (A) Multivariate Cox analysis in TCGA training set. (B) Multivariate Cox analysis in the GSE32062 validation set. (C) Nomogram of clinical features and risk score. (D) Calibration plot of 1-, 3-, and 5-years. (E) Risk score differences in age, status, stage and grade subgroups. $^*p < 0.05$; $^{**}p < 0.01$ and $^{****}p < 0.0001$; ns, not significant.

(**Supplementary Fig. 6**).

more active (**Supplementary Fig. 7A**).

3.6 GSVA Analysis

Significantly enriched pathways were calculated using the R package "limma" and screened on the condition of FDR <0.05. A total of 103 metabolic pathways were screened out. The top 10 pathways were selected from the high- and the low-risk groups, respectively. Some metabolic pathways, such as ECM receptor interaction, focal adhesion and axon guidance were more active in the high-risk group; while in the low-risk group, proteasome, DNA replication, spliceosome, protein export, aminoacyl TRNA biosynthesis and other metabolic pathways were

3.7 DEGs and GO Enrichment Analysis

The cancer tissue samples were grouped according to the risk score in TCGA dataset and DEG analysis was performed. Finally, 158 DEGs were screened, of which 102 upregulated genes and 56 downregulated genes were identified (**Supplementary Fig. 7B**). DAVID was used to analyze the function of the DEGs under the screening threshold of FDR <0.05. GO enrichment analysis revealed that the DEGs were mainly enriched in the extracellular region under cellular component (CC). As regards molecular function (MF), the DEGs were mainly enriched in colla-
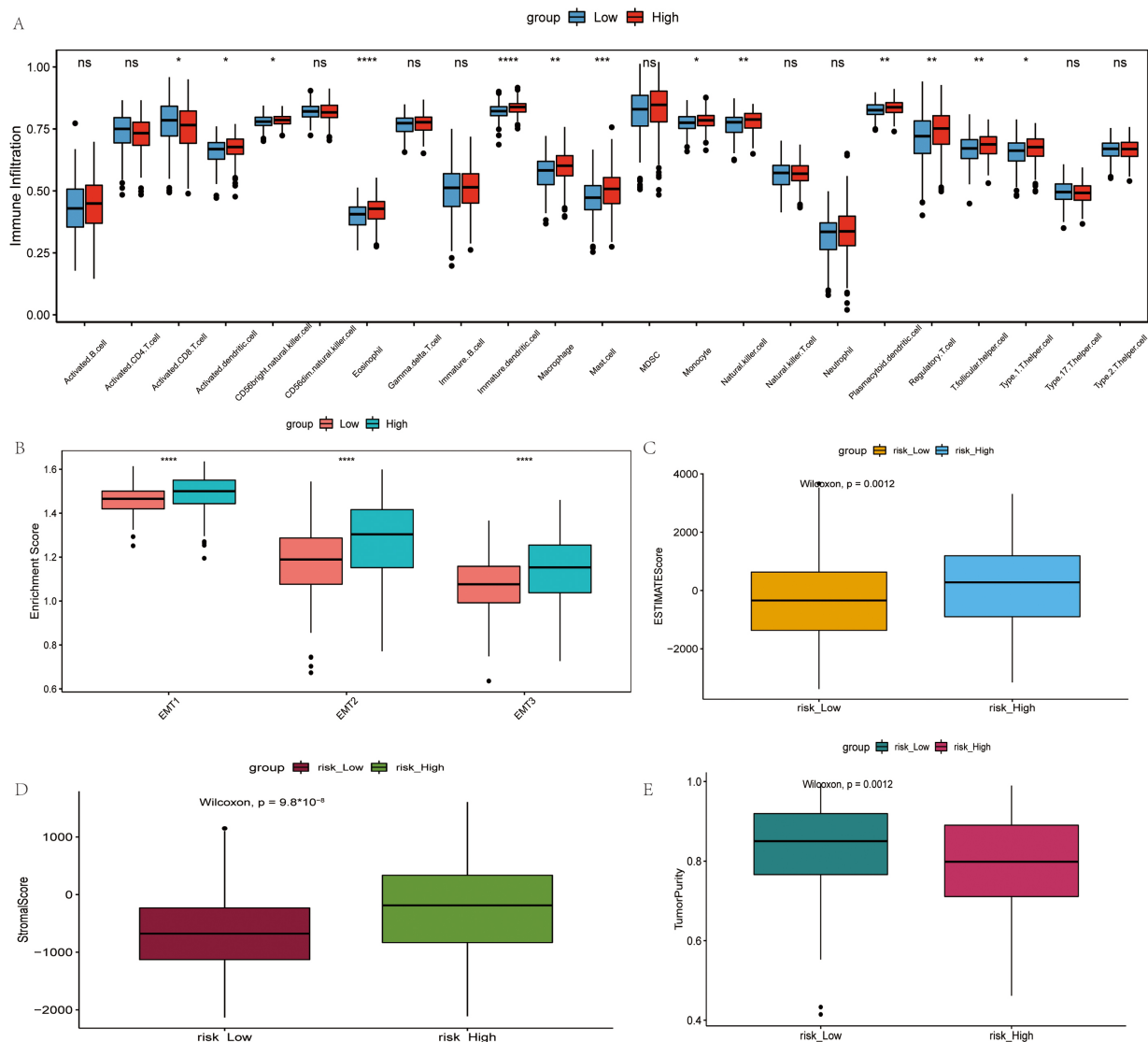
Fig. 5. Comparison of the immune microenvironment in the high- and low-risk groups. (A) Difference in the infiltration degree of 23 types of immune cells. Red and blue represent high-risk and low-risk groups, respectively. (B) Difference in infiltration degree of EMT, green and pink represent high-risk and low-risk groups, respectively. (C) Difference in ESTIMATE score, orange and blue represent high-risk and low-risk groups, respectively. (D) Difference in stromal score, brown and blue represent high-risk and low-risk groups, respectively. (E) Difference in tumor purity, purple and green represent high-risk and low-risk groups, respectively. $^*p < 0.05$; $^{**}p < 0.01$; $^{***}p < 0.001$ and $^{****}p < 0.0001$; ns, not significant.

gen binding. In terms of biological process (BP), the DEGs were significantly enriched in the type I interferon signaling pathway, as shown in **Supplementary Fig. 7C**.

3.8 Association between TMB and Risk Score

It was considered meaningful to explore the inner link between the risk score and TMB in order to elucidate the genetic characteristic of each subgroup. Kaplan-Meier analysis of the survival curve revealed that the high-TMB group had a longer survival rate. The increase in the TMB level led to an improvement in survival, while the low-risk and high-TMB group survived the longest (Fig. 6A,B). There was no significant difference in TMB between the high- and

low risk groups (Fig. 6C). Furthermore, there is no correlation between risk score and TMB (Fig. 6E). A high TMB induces antitumor immune cell activation and improves the prognosis of patients with OV.

3.9 Immune Checkpoints and Immunological Therapy

The expression of immune checkpoints, including *CD274*, *CTLA4*, *KLRC1*, *LAG3*, *PDCD1* and *TIGIT* was assessed in the high- and low-risk groups, followed by the evaluation of the relevance between these immune checkpoints, and risk score and signature genes. In the low-risk group, *CD274*, *CTLA4*, *KLRC1*, *LAG3* and *PDCD1* were significantly highly expressed. *GZMB* exhibited a positive
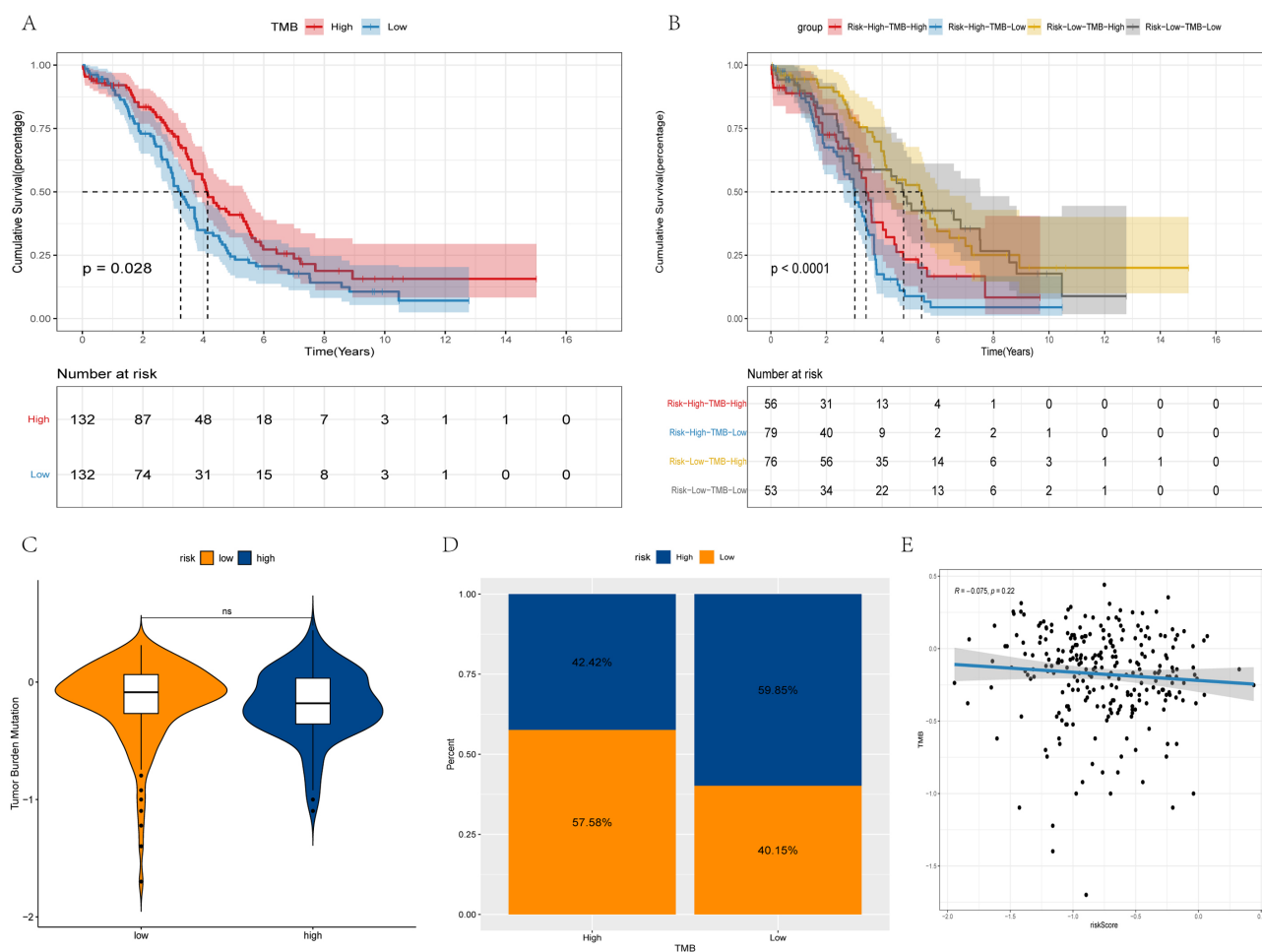
Fig. 6. Differences in TMB between high and low-risk groups. (A,B) Survival curves of the different groups. (C) Violin plot of TMB. (D) Bar chart of proportional distribution. (E) Correlation between TMB and risk score.

association with each immune checkpoint, while the risk score was negatively associated with each immune checkpoint (Fig. 7A,B).

Immunotherapy represented by the blocking of programmed cell death ligand 1 (PD-L1) and programmed cell death 1 (PD-1) has become a key breakthrough in the treatment of cancer. The present study then investigated whether the risk score can forecast the response of patients to immune checkpoint blockade treatment based on an immunotherapy cohort. In the anti-PD-L1 cohort, patients demonstrated significant clinical benefits and a notable prolonged survival was observed in the low-risk group (Fig. 7D). The therapeutic advantage was confirmed in the low-risk patients (Fig. 7D–F). Finally, the ability of the risk score to distinguish between the disease progression group (PD/SD) and disease remission group (CR/PR) treated with anti-PD-L1 immunotherapy was examined using the ROC curve (Fig. 7G). Overall, the findings of the present study strongly suggest that the risk score is significantly associated with the tumor response to immunotherapy. The risk score established herein may contribute to the prediction of the response to immunotherapy.

4. Discussion

OV is a malignant ovarian tumor; 90–95% of cases are primary OV, and the remaining 5–10% cases are metastatic, with the tumor in the ovaries originating from a primary tumor elsewhere in the body. Diagnosis is difficult in the early stages of OV [30]. Among the gynecological malignancies, the high mortality rate associated with OV poses a severe threat to the lives of women [31].

In the present study, a risk score model was constructed consisting of 10 IRGs and FRGs (*C5AR1*, *GZMB*, *IGF2R*, *ISG20*, *PPP3CA*, *STAT1*, *TRIM27*, *TSHR*, *RB1* and *EGFR*), which can predict the prognosis of patients with OV. Some genes were involved in pathophysiological features of OV. *GZMB* is a serine protease with the highest content secreted by cytotoxic T-lymphocytes and natural killer cells [32]. Previous studies have demonstrated that *GZMB* is detected in lung carcinomas [33], primary breast carcinomas [34], urothelial carcinomas [35] and nasal-type NK/T-cell lymphoma [36]. Wang *et al*. [37] demonstrated that *GZMB* was associated with OS and could affect prognosis through its effect on immune cell infiltra-
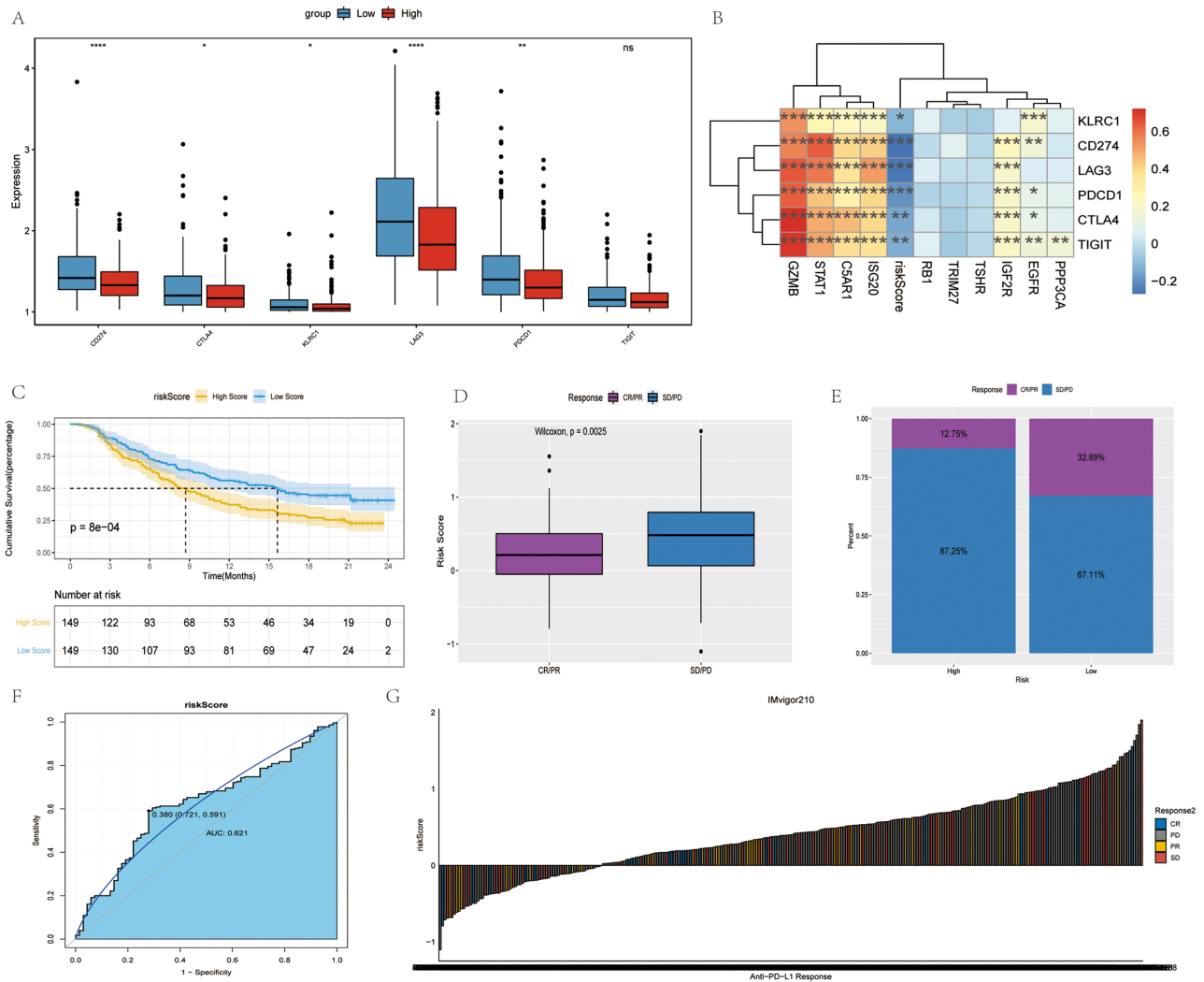
Fig. 7. Immune checkpoints and anti-PD-1/L1 immunotherapy. (A) Differences in immune checkpoints between high- and low- risk groups. Red and blue represent high-risk and low-risk groups, respectively. (B) Correlation analysis of immune checkpoints. (C) Survival curves of high- and low- risk groups. (D) Differences in risk scores between different anti-PD-1 clinical response groups. (E) Proportion of patients responding to anti-PD-1/L1 immunotherapy in high- and low- risk groups. (F) Accuracy of risk score in differentiating the PD/SD and CR/PR groups. (G) Correlation of risk score with clinical response to anti-PD-1/L1 immunotherapy. $^{*}p < 0.05$; $^{**}p < 0.01$; $^{***}p < 0.001$ and $^{****}p < 0.0001$; ns, not significant. SD, stable disease; PD, progressive disease; CR, complete response; PR, partial response.

tion, thus being a potential target for immunotherapy of OV. The expression of *ISG20* is associated with a variety of chemokines, resulting in the infiltration of various immune cells into tumors, and the level of *ISG20* is positively related to the expression of PD-1/PD-L1 and CTLA4, which further inhibits T-cell function, resulting in tumor evasion to the immune response [38]. The overexpression of *STAT1* has been shown to attenuate the TGF-β signaling pathway in OV cells, implying that the high expression of *STAT1* may be beneficial to the OS of patients with OV [39]; this is consistent with the results of the present study. *EGFR* can activate a variety of downstream signaling pathways, thereby promoting the proliferation, invasion and metastasis of tumor cells [40]. Tang *et al.* [41] found *PPP3CA* was

associated with a poor survival of patients with cholangiocarcinoma. In summary, the expression of prognostic genes is associated with OV. It was hypothesized that highly expressed genes were associated with the occurrence of OV, and that genes expressed at low levels were involved in the development of OV. Each gene does not function alone, and may interact with other genes [42].

The independence of the risk score remained robust in the training and validation sets. The nomogram constructed by the combined model could better predict the short-term survival of patients with OV than a single prognostic factor. The OS of patients in the high-risk group was significantly lower than that of those in the low-risk group.

In addition, the present study screened out drugs re-

lated to antitumor and immunotherapy. Sunitinib has been shown to suppress the migration of OV cells through the negative modulation of TGF-β-mediated EMT [43]. Palbociclib, a member of a class of drugs known as CDK4/6 inhibitors, can disrupt the proliferation of cancer cells and treat recurrent OV [44]; tacrolimus is a potent new immunosuppressant that inhibits the release of IL-2 and comprehensively inhibits the action of T-lymphocytes. Sirolimus inhibits the expression of hypoxia-inducible factor 1α and tumor growth in a SKOV3 OV model [45].

Furthermore, in the present study, in the high-risk group, a greater number of immune cells were infiltrated. However, the OS of patients in the high-risk group was significantly lower. Macrophages (TAMs) and regulatory T-cells (Tregs) promote OV immune surveillance evasion and tumor transfer. Immune cells in immune-rejecting tumors reside in the stroma surrounding tumor cells, instead of penetrating the tumor. The activation of the stroma in the TIME is considered to be associated with T-cell suppression [46,47]. Therefore, it was hypothesized that stromal activation inhibited the antitumor function of immunocytes in the high-risk group. EMT is a key process in cancer progression and metastasis, promoting OV invasion [48]. In addition, in the present study, the ESTIMATE score and stromal score were significantly higher in the high-risk group, although the tumor purity was low, which is in line with the findings of previous studies [49–53]. Low tumor purity and a high stroma infiltrates were negatively associated with a shorter survival [54].

TMB is a hallmark of immunotherapy due to the biological mechanisms and immune responses to somatic mutations [55–58]. That is, mutations in neoantigens increase when the TMB is higher. It is easier for the immune system to recognize and remove tumor cells. In addition, the survival rate of patients will be improved. The OS of patients with OV with a high TMB is significantly increased [59]. Herein, the combined analysis of the TMB and risk score found that patients with a high TMB and a low risk score had the best prognosis, while those with a low TMB and a high risk score had the worst prognosis. This implies that the risk score and TMB may play a role in different aspects of OV immunotherapy. This statement is also confirmed by the lack of a correlation between the risk score and TMB.

Immune checkpoints regulate the degree of immune activation and prevent the immune system from overactivation. This regulatory mechanism maintains the immune response within the normal physiological range and protects the host against autoimmunity. Based on immune checkpoint analysis, the present study found that *CD274*, *CTLA4*, *KLRC1*, *LAG3* and *PDCD1* were overexpressed in the low-risk group. Tu *et al*. [60] assessed the expression and therapeutic response of PD-1 in different types of cancer. Notably, the upregulation of PD-1 expression had a positive effect on OV, and the OS of patients with OV with an upregulated expression of *CTLA4* was improved. The inhibitory

checkpoint targets may be more efficient in patients with a high risk score in OV [61]. In addition, immune checkpoints were inversely associated with higher risk scores. Using the risk score to predict biological response to anti-immunotherapy in tumor samples may be helpful for OV immunotherapy. In the present study, patients in the low-risk group demonstrated significant clinical benefits and a significantly prolonged survival.

However, there are limitations to the study. Firstly, this study was carried out by using bioinformatics analysis. Although we verified the expression of the genes by RT-PCR *in vitro*, the sample size is relatively small. In the later stage, the sample size can be increased. Secondly, some various experiments are needed to make the results more convincing, such as cell and animal models experiments. Lastly, the association between clinical value and immunotherapy are needed to further investigate in prospective trials.

5. Conclusions

In conclusion, the present study constructed a 10-gene risk model that can function as an independent prognostic factor in patients with OV and predict the response to immunotherapy. In addition, the findings obtained may still provide a rational basis for the study of immunotherapy in OV, and the identified signature genes may provide aid future research in OV.

Availability of Data and Materials

All data generated or analyzed during this study are included in this published article.

Author Contributions

CW designed the research study. GZ performed the research. MG, YL, PL and TC provided help and advice on CW analyzed the data. CW wrote the manuscript. All authors contributed to editorial changes in the manuscript. All authors read and approved the final manuscript.

Ethics Approval and Consent to Participate

The Ethics Committee of the Second Affiliated Hospital of Xi'an Jiaotong University approved this study (2021241). Patient informed consent was obtained.

Acknowledgment

Not applicable.

IMR Press

Conflict of Interest

The authors declare no conflict of interest.

Supplementary Material

Supplementary material associated with this article can be found, in the online version, at https://doi.org/10.31083/j.fbl2801004.

References

[1] Bray F, Ferlay J, Soerjomataram I, Siegel RL, Torre LA, Jemal A. Global cancer statistics 2018: GLOBOCAN estimates of incidence and mortality worldwide for 36 cancers in 185 countries. CA: A Cancer Journal for Clinicians. 2018; 68: 394–424.

[2] Lheureux S, Gourley C, Vergote I, Oza AM. Epithelial ovarian cancer. The Lancet. 2019; 393: 1240–1253.

[3] Henley SJ, Ward EM, Scott S, Ma J, Anderson RN, Firth AU, et al. Annual report to the nation on the status of cancer, part i: National cancer statistics. Cancer. 2020; 126: 2225–2249.

[4] Matulonis UA, Sood AK, Fallowfield L, Howitt BE, Sehouli J, Karlan BY. Ovarian cancer. Nature Reviews Disease Primers. 2016; 2: 16061.

[5] Lee J, Kim S, Kim YT, Lim MC, Lee B, Jung K, et al. Changes in ovarian cancer survival during the 20 years before the era of targeted therapy. BMC Cancer. 2018; 18: 601.

[6] Ding Q, Dong S, Wang R, Zhang K, Wang H, Zhou X, et al. A nine-gene signature related to tumor microenvironment predicts overall survival with ovarian cancer. Aging. 2020; 12: 4879–4895.

[7] Zheng M, Hu Y, Gou R, Nie X, Li X, Liu J, et al. Identification three LncRNA prognostic signature of ovarian cancer based on genome-wide copy number variation. Biomedicine & Pharmacotherapy. 2020; 124: 109810.

[8] Sun H, Cao D, Ma X, Yang J, Peng P, Yu M, et al. Identification of a Prognostic Signature Associated With DNA Repair Genes in Ovarian Cancer. Frontiers in Genetics. 2019; 10: 839.

[9] Ye Y, Dai Q, Li S, He J, Qi H. A Novel Defined Risk Signature of the Ferroptosis-Related Genes for Predicting the Prognosis of Ovarian Cancer. Frontiers in Molecular Biosciences. 2021; 8: 645845.

[10] Verbon EH, Trapet PL, Stringlis IA, Kruijs S, Bakker PAHM, Pieterse CMJ. Iron and Immunity. Annual Review of Phytopathology. 2017; 55: 355–375.

[11] Hassannia B, Vandenabeele P, Vanden Berghe T. Targeting Ferroptosis to Iron out Cancer. Cancer Cell. 2019; 35: 830–849.

[12] Liang C, Zhang X, Yang M, Dong X. Recent Progress in Ferroptosis Inducers for Cancer Therapy. Advanced Materials. 2019; 31: 1904197.

[13] Basuli D, Tesfay L, Deng Z, Paul B, Yamamoto Y, Ning G, et al. Iron addiction: a novel therapeutic target in ovarian cancer. Oncogene. 2017; 36: 4089–4099.

[14] You Y, Fan Q, Huang J, Wu Y, Lin H, Zhang Q. Ferroptosis-Related Gene Signature Promotes Ovarian Cancer by Influencing Immune Infiltration and Invasion. Journal of Oncology. 2021; 2021: 9915312.

[15] Gentles AJ, Newman AM, Liu CL, Bratman SV, Feng W, Kim D, et al. The prognostic landscape of genes and infiltrating immune cells across human cancers. Nature Medicine. 2015; 21: 938–945.

[16] Angell H, Galon J. From the immune contexture to the Immunoscore: the role of prognostic and predictive immune markers in cancer. Current Opinion in Immunology. 2013; 25: 261–267.

[17] Kandalaft LE, Powell DJ, Singh N, Coukos G. Immunotherapy for Ovarian Cancer: what's next? Journal of Clinical Oncology. 2011; 29: 925–933.

[18] Kershaw MH, Westwood JA, Parker LL, Wang G, Eshhar Z, Mavroukakis SA, et al. A Phase i Study on Adoptive Immunotherapy Using Gene-Modified T Cells for Ovarian Cancer. Clinical Cancer Research. 2006; 12: 6106–6115.

[19] Goodell V, Salazar LG, Urban N, Drescher CW, Gray H, Swensen RE, et al. Antibody Immunity to the p53 Oncogenic Protein is a Prognostic Indicator in Ovarian Cancer. Journal of Clinical Oncology. 2006; 24: 762–768.

[20] Doo DW, Norian LA, Arend RC. Checkpoint inhibitors in ovarian cancer: a review of preclinical data. Gynecologic Oncology Reports. 2019; 29: 48–54.

[21] Wang W, Liu JR, Zou W. Immunotherapy in Ovarian Cancer. Surgical Oncology Clinics of North America. 2019; 28: 447–464.

[22] Wang W, Green M, Choi JE, Gijón M, Kennedy PD, Johnson JK, et al. CD8+ T cells regulate tumour ferroptosis during cancer immunotherapy. Nature. 2019; 569: 270–274.

[23] Liang J, Wang D, Lin H, Chen X, Yang H, Zheng Y, et al. A Novel Ferroptosis-related Gene Signature for Overall Survival Prediction in Patients with Hepatocellular Carcinoma. International Journal of Biological Sciences. 2020; 16: 2430–2441.

[24] Charoentong P, Finotello F, Angelova M, Mayer C, Efremova M, Rieder D, et al. Pan-cancer Immunogenomic Analyses Reveal Genotype-Immunophenotype Relationships and Predictors of Response to Checkpoint Blockade. Cell Reports. 2017; 18: 248–262.

[25] Barbie DA, Tamayo P, Boehm JS, Kim SY, Moody SE, Dunn IF, et al. Systematic RNA interference reveals that oncogenic KRAS-driven cancers require TBK1. Nature. 2009; 462: 108–112.

[26] Liu Y, Zhu K, Guan X, Xie S, Wang Y, Tong Y, et al. TTK is a potential therapeutic target for cisplatin-resistant ovarian cancer. Journal of Ovarian Research. 2021; 14: 128.

[27] Boyd LR, Muggia FM. Carboplatin/Paclitaxel Induction in Ovarian Cancer: The Finer Points. Oncology. 2018; 32: 418–420, 422–424.

[28] Silva F, Félix A, Serpa J. Functional redundancy of the Notch pathway in ovarian cancer cell lines. Oncology Letters. 2016; 12: 2686–2691.

[29] Wen K, Yan Y, Shi J, Hu L, Wang W, Liao H, et al. Construction and Validation of a Combined Ferroptosis and Hypoxia Prognostic Signature for Hepatocellular Carcinoma. Frontiers in Molecular Biosciences. 2021; 8: 809672.

[30] Mi JL, Xu M, Liu C, Wang RS. Interactions between tumor mutation burden and immune infiltration in ovarian cancer. International Journal of Clinical and Experimental Pathology. 2020; 13: 2513–2523.

[31] Nie X, Song L, Li X, Wang Y, Qu B. Prognostic signature of ovarian cancer based on 14 tumor microenvironment-related genes. Medicine. 2021; 100: e26574.

[32] Krepela. Granzyme B-induced apoptosis in cancer cells and its regulation (Review). International Journal of Oncology. 2010; 37: 1361–1378.

[33] Kontani K, Sawai S, Hanaoka J, Tezuka N, Inoue S, Fujino S. Involvement of granzyme B and perforin in suppressing nodal metastasis of cancer cells in breast and lung cancers. European Journal of Surgical Oncology. 2001; 27: 180–186.

[34] Hu SX, Wang S, Wang JP, Mills GB, Zhou Y, Xu H. Expression of endogenous granzyme B in a subset of human primary breast carcinomas. British Journal of Cancer. 2003; 89: 135–139.

[35] D'Eliseo D, Pisu P, Romano C, Tubaro A, De Nunzio C, Morrone S, et al. Granzyme B is expressed in urothelial carcinoma and promotes cancer cell invasion. International Journal of Cancer. 2010; 127: 1283–1294.

[36] Ko Y, Park S, Jin H, Woo H, Lee H, Park C, et al. Granzyme B

leakage-induced apoptosis is a crucial mechanism of cell death in nasal-type NK/T-cell lymphoma. Laboratory Investigation. 2007; 87: 241–250.

[37] Wang J, Su X, Wang C, Xu M. Integrated analysis of prognostic immune-related genes in the tumor microenvironment of ovarian cancer. Annals of Translational Medicine. 2022; 10: 91–91.

[38] Keir ME, Butte MJ, Freeman GJ, Sharpe AH. PD-1 and its Ligands in Tolerance and Immunity. Annual Review of Immunology. 2008; 26: 677–704.

[39] Zhang J, Wang F, Liu F, Xu G. Predicting STAT1 as a prognostic marker in patients with solid cancer. Therapeutic Advances in Medical Oncology. 2020; 12: 175883592091755.

[40] Granados ML, Hudson LG, Samudio-Ruiz SL. Contributions of the Epidermal Growth Factor Receptor to Acquisition of Platinum Resistance in Ovarian Cancer Cells. PLoS ONE. 2015; 10: e0136893.

[41] Tang Z, Yang Y, Zhang J, Fu W, Lin Y, Su G, et al. Quantitative Proteomic Analysis and Evaluation of the Potential Prognostic Biomarkers in Cholangiocarcinoma. Journal of Cancer. 2019; 10: 3985–3999.

[42] Bao M, Zhang L, Hu Y. Novel gene signatures for prognosis prediction in ovarian cancer. Journal of Cellular and Molecular Medicine. 2020; 24: 9972–9984.

[43] Chen ZB, Chang LL, Zhou TY, Wang DD, Chen Y, Zhao PG, et al. Sunitinib suppresses migration of ovarian cancer cells through negative modulation of TGF-β-mediated epithelial-mesenchymal transition. Zhejiang Da Xue Xue Bao Yi Xue Ban. 2015; 44: 479–485. (In Chinese)

[44] Lee DW, Ho GF. Palbociclib in the treatment of recurrent ovarian cancer. Gynecologic Oncology Reports. 2020; 34: 100626.

[45] Sung H, Ferlay J, Siegel RL, Laversanne M, Soerjomataram I, Jemal A, et al. Global Cancer Statistics 2020: GLOBOCAN Estimates of Incidence and Mortality Worldwide for 36 Cancers in 185 Countries. CA: a Cancer Journal for Clinicians. 2021; 71: 209–249.

[46] Zhang B, Wu Q, Li B, Wang D, Wang L, Zhou YL. M6a regulator-mediated methylation modification patterns and tumor microenvironment infiltration characterization in gastric cancer. Molecular Cancer. 2020; 19: 53.

[47] Chen DS, Mellman I. Elements of cancer immunity and the cancer–immune set point. Nature. 2017; 541: 321–330.

[48] Fan L, Lei H, Zhang S, Peng Y, Fu C, Shu G, et al. Non-canonical signaling pathway of SNAI2 induces EMT in ovarian cancer cells by suppressing miR-222-3p transcription and upregulating PDCD10. Theranostics. 2020; 10: 5895–5913.

[49] Mesker WE, Junggeburt JM, Szuhai K, de Heer P, Morreau H, Tanke HJ, et al. The carcinoma-stromal ratio of colon carcinoma is an independent factor for survival compared to lymph node status and tumor stage. Cellular Oncology. 2007; 29: 387–398.

[50] West NP, Dattani M, McShane P, Hutchins G, Grabsch J, Mueller W, et al. The proportion of tumour cells is an independent predictor for survival in colorectal cancer patients. British Journal of Cancer. 2010; 102: 1519–1523.

[51] Huijbers A, Tollenaar RAEM, v Pelt GW, Zeestraten ECM, Dutton S, McConkey CC, et al. The proportion of tumor-stroma as a strong prognosticator for stage II and III colon cancer patients: validation in the VICTOR trial. Annals of Oncology. 2013; 24: 179–185.

[52] van Wyk HC, Roseweir A, Alexander P, Park JH, Horgan PG, McMillan DC, et al. The Relationship between Tumor Budding, Tumor Microenvironment, and Survival in Patients with Primary Operable Colorectal Cancer. Annals of Surgical Oncology. 2019; 26: 4397–4404.

[53] Danielsen HE, Hveem TS, Domingo E, Pradhan M, Kleppe A, Syvertsen RA, et al. Prognostic markers for colorectal cancer: estimating ploidy and stroma. Annals of Oncology. 2018; 29: 616–623.

[54] Mao Y, Feng Q, Zheng P, Yang L, Liu T, Xu Y, et al. Low tumor purity is associated with poor prognosis, heavy mutation burden, and intense immune phenotype in colon cancer. Cancer Management and Research. 2018; 10: 3569–3577.

[55] Gubin MM, Zhang X, Schuster H, Caron E, Ward JP, Noguchi T, et al. Checkpoint blockade cancer immunotherapy targets tumour-specific mutant antigens. Nature. 2014; 515: 577–581.

[56] Birkbak NJ, Kochupurakkal B, Izarzugaza JM, Eklund AC, Li Y, Liu J, et al. Tumor mutation burden forecasts outcome in ovarian cancer with BRCA1 or BRCA2 mutations. PLoS ONE. 2013; 8: e80023.

[57] Chan TA, Yarchoan M, Jaffee E, Swanton C, Quezada SA, Stenzinger A, et al. Development of tumor mutation burden as an immunotherapy biomarker: utility for the oncology clinic. Annals of Oncology. 2019; 30: 44–56.

[58] Nadal E, Massuti B, Dómine M, García-Campelo R, Cobo M, Felip E. Immunotherapy with checkpoint inhibitors in non-small cell lung cancer: insights from long-term survivors. Cancer Immunology, Immunotherapy. 2019; 68: 341–352.

[59] Cui M, Xia Q, Zhang X, Yan W, Meng D, Xie S, et al. Development and Validation of a Tumor Mutation Burden-Related Immune Prognostic Signature for Ovarian Cancers. Frontiers in Genetics. 2022; 12: 688207.

[60] Tu L, Guan R, Yang H, Zhou Y, Hong W, Ma L, et al. Assessment of the expression of the immune checkpoint molecules PD-1, CTLA4, TIM-3 and LAG-3 across different cancers in relation to treatment response, tumor-infiltrating immune cells and survival. International Journal of Cancer. 2020; 147: 423–439.

[61] Gao Y, Chen L, Cai G, Xiong X, Wu Y, Ma D, et al. Heterogeneity of immune microenvironment in ovarian cancer and its clinical significance: a retrospective study. Oncoimmunology. 2020; 9: 1760067.